research articles Journal of proteome research

Secreted Proteome Profiling in Human RPE Cell Cultures Derived from Donors with Age Related Macular Degeneration and Age Matched Healthy Donors

Eunkyung An,[†,‡] Xiaoning Lu,[†] Jessica Flippin,[†] Joseph M. Devaney,[†] Brian Halligan,[§] Eric Hoffman,[†] Karl Csaky,[||] and Yetrib Hathout*[,†]

Center for Genetic Medicine, Children's National Medical Center, Washington, DC, Program in Biochemistry and Molecular Genetics, Institute of Biomedical Science, The George Washington University, Washington, DC, Bioinformatics, Human and Molecular Genetics Center, Medical College of Wisconsin, Milwaukee, Wisconsin, and National Eye Institute, National Institute of Health, Bethesda, Maryland

Received March 27, 2006

Age-related macular degeneration (AMD) is characterized by progressive loss of central vision, which is attributed to abnormal accumulation of macular deposits called "drusen" at the interface between the basal surface of the retinal pigment epithelium (RPE) and Bruch's membrane. In the most severe cases, drusen deposits are accompanied by the growth of new blood vessels that breach the RPE layer and invade photoreceptors. In this study, we hypothesized that RPE secreted proteins are responsible for drusen formation and choroidal neovascularization. We used stable isotope labeling by amino acids in cell culture (SILAC) in combination with LC−MS/MS analysis and ZoomQuant quantification to assess differential protein secretion by RPE cell cultures prepared from human autopsy eyes of AMD donors (diagnosed by histological examinations of the macula and genotyped for the Y402H-complement factor H variant) and age-matched healthy control donors. In general, RPE cells were found to secrete a variety of extracellular matrix proteins, complement factors, and protease inhibitors that have been reported to be major constituents of drusen (hallmark deposits in AMD). Interestingly, RPE cells from AMD donors secreted 2 to 3-fold more galectin 3 binding protein, fibronectin, clusterin, matrix metalloproteinase-2 and pigment epithelium derived factor than RPE cells from age-matched healthy donors. Conversely, secreted protein acidic and rich in cysteine (SPARC) was found to be down regulated by 2-fold in AMD RPE cells versus healthy RPE cells. Ingenuity pathway analysis grouped these differentially secreted proteins into two groups; those involved in tissue development and angiogenesis and those involved in complement regulation and protein aggregation such as clusterin. Overall, these data strongly suggest that RPE cells are involved in the biogenesis of drusen and the pathology of AMD.

Keywords: AMD • retinal pigment epithelial cells • drusen • SILAC • secreted proteins • clusterin • complement factor H • SPARC

Introduction

Age-related macular degeneration (AMD) is a leading cause of blindness in the elderly population.[1] Currently, there is no effective cure for the disease due to a lack of therapeutic targets. AMD is characterized by proteinaceous deposits called "drusen" that accumulate between the retinal pigment epithelium (RPE) and Bruch's membrane.[2−4] An increase in the number and volume of these drusen is indicative of progressive AMD.[5−7] There are two forms of AMD: dry atrophic without neovascularization and wet with exudative neovascularization. The genetic predisposition to both forms has recently begun to be elucidated. Indeed, four independent groups have clearly demonstrated that a complement factor H polymorphism (Y402H−CFH) is strongly associated with the risk of developing AMD.[8−11] Additional recent studies have implicated gene variants of complement factor B and complement 2, whose protein products are involved in the same pathway as complement factor H.[12] Although genetic factors of the disease are being unraveled, the pathophysiology remains difficult to understand. Specifically, the formation of the characteristic drusen and choroidal neovascularizton (CNV) in the retina is not well understood. It has been long hypothesized that RPE may play a primary role in the formation of drusen.[13] The RPE is composed of highly specialized and active phagocytic epithelial cells localized between the photoreceptors and choroids. These cells perform crucial functions in the eye, such as daily phagocytosis of fragments shed from rod and cone cells,

* To whom correspondence should be addressed: Yetrib Hathout; Tel: (202) 884−3136; Fax: (202) 884−6014; E-mail: yhathout@cnmcresearch.org.
[†] Children's National Medical Center.
[‡] The George Washington University.
[§] Medical College of Wisconsin.
[||] National Eye Institute.

10.1021/pr060121j CCC: $33.50

Published on Web 08/24/2006

processing and transport of nutrients, and recycling of visual pigments.[14] Unfortunately, these post-mitotic cells are vulnerable to aging effects and deteriorate with time, resulting in progressive degeneration.

In this study, we hypothesized that abnormal protein secretion by RPE cells might be involved in drusen and CNV formation in AMD patients, resulting in progressive degeneration of the retina and loss of vision. RPE cells are known to secrete a variety of proteins such as growth factors[15] and protease inhibitors[16,17] and are a source of the vascular endothelial growth factor involved in diabetic retinopathy.[18,19] Thus, profiling and cataloguing proteins secreted by RPE cells may provide insight into their role in AMD.

Stable isotope labeling by amino acids in cell culture (SILAC) is becoming the method of choice for protein profiling when using cell culture systems.[20,21] Because labeled and unlabeled cells can be mixed before protein extraction, variations in protein ratios resulting from sample processing and handling are minimized. This method has been successfully used to accurately determine protein ratios between samples representing different biological states[22−24] and is suitable to study the phosphoproteome in cell culture systems[25−27] as well as protein−protein interactions.[28,29] More recently, SILAC was used to study and characterize secreted proteins in a pancreatic cancer cell line in search for potential pancreatic cancer biomarkers.[30] We implemented a similar strategy to examine differential protein secretion, "secretome profiling", in primary human RPE cell cultures prepared from AMD donors and age-matched healthy donors.

Experimental Method

Preparation of Primary RPE Cell Culture from Postmortem Autopsy Eyes. Donor's eyes were received through Heartland Lions Eye Bank (eyes are collected within a few hours (4−6) after death and shipped in sterile physiologic solution). The average donor age was 65 years old and above, including both females and males. The anterior segment from each donor eye was removed by cutting around the iris and removing it along with the lens. A biopsy was then taken from the macula of each eye for histological examination by electron microscopy (EM). RPE cells were harvested from the remaining tissue according to previously published procedures[31] with some modifications. Briefly, the vitrous and the retina were carefully peeled away from the RPE-choroid-sclera using fine forceps. Then the RPE-choroid was carefully separated from the sclera and placed face up in a small sterile Petri dish. Then, 0.1% dispase (Roche, Indianapolis, IN) prepared in Ca^{2+} and Mg^{2+}-free Hank's balanced salt solution was added to completely cover the tissue. After incubation at 37 °C for about 3 h with occasional shaking, the liquid was carefully aspirated and transferred to a sterile centrifuge tube. The suspension was then centrifuged at 300 × g for 5 min, and the cell pellet was resuspended gently in Dulbecco's modified Eagle's medium DMEM/F12 (Invitrogen, Carlsbad, CA) supplemented with 10% FBS (Invitrogen, Carlsbad, CA), 100 U/mL penicillin, and 100 μg/mL streptomycin. The suspended cells were then transferred to T25 culture flasks and placed in an incubator at 37 °C and 5% CO_2 under humidified atmosphere. Growing cells were tested for their epithelial content using an established immunohistochemical staining for cytokeratins.[32]

Screening RPE Cell Cultures for the Y402H CFH Variant. DNA was extracted from each of the RPE cultures obtained above and screened for the Y402H−CFH polymorphism (rs1061170). An allelic discrimination assay (TaqMan assay)[33] was used to detect homozygous mutant rare allele (CC), heterozygous (CT) and wild type genotypes in CFH gene. The assay uses two TaqMan probes that differ at the polymorphic site, with one probe complementary to the wild-type allele and the other to the variant allele. The probes contained different fluorescent reporter dyes (VIC and FAM) to differentiate the amplification of each allele. A quencher dye is covalently linked to the wild-type or variant allele probes. When the probes are intact, fluorescence is quenched because of the physical proximity of the reporter and quencher dyes. During the PCR annealing step, the TaqMan probes hybridize to the targeted polymorphic site. During the PCR extension phase, the reporter dye is cleaved by the nuclease activity of the Taq polymerase, leading to an increase in the characteristic fluorescence of the reporter dye. The signal generated by PCR amplification indicates the alleles that are present in the sample. Specific genotyping is determined by measuring the signal intensity of the two different reporter dyes after the PCR reaction.

An allele-specific PCR reaction was used for each single nucleotide polymorphism (SNP) including 20 ng genomic DNA, 900 nM forward and reverse PCR primers (F: 5′- CTTTATT-TATTTATCATTGTTATGGTCCTTAGGAAAATGTTATTT-3′ and R: 5′- GGCAGGCAACGTCTATAGATTTACC-3′), 200 nM fluorescent allele discrimination probes (WT: VIC-5′-TTTCTTC-CATAATTTTG-3′; MT (rare allele: VIC-5′-TTTCTTCCATGATTTTG-3′) and TaqMan Universal PCR Master Mix, No AmpErase UNG (Applied Biosystems, Foster City, CA) in a final volume of 10 μL. The PCR was preformed at 95 °C for 10 min and 44 cycles of 15 s at 92 °C and 1 min at an annealing temperature of 60 °C. Reactions were set up using a MWG robot, and fluorescence ratios and allele calling measured using an ABI 7900.

Stable Isotope Labeling by Amino Acids. A suspension of RPE cells (about 150 000 cells) with the wild-type CFH genotype (TT-RPE) prepared from an eye of a healthy donor was incubated in custom-made DMEM/F12 medium without Arg nor Lys (Atlanta Biologicals, Lawrenceville, GA) to which the following were added: 10% FBS (Invitrogen, Carlsbad, CA), 100 U/mL each of penicillin and streptomycin, $^{13}C_6$−Arg (147.5 μg/mL), and $^{13}C_6$, $^{15}N_2$−Lys (91.25 μg/mL) (Cambridge Isotope Laboratories, Inc., Andover, MA). In parallel, the same amount of RPE cells were prepared from AMD donors with the homozygous rare CFH genotype (CC-RPE) and the heterozygous CFH genotype (CT-RPE) were grown in the same media containing unlabeled L-Arg and L-Lys instead of isotopically labeled ones. All RPE cells were sub-cultured to passage 4. After confluence, cells were washed five times with PBS buffer to remove excess bovine serum proteins and then incubated in serum-free labeled and unlabeled media for a period of 18 h.

Sample Preparation of Secreted Proteins. Spent media from each of the labeled and unlabeled RPE cultures were collected in 15 mL tubes (BD Biosciences Falcon, San Jose, CA) and then filtered through a 0.22 μm nylon filter (Millipore, Bedford, MA). The filtrate was centrifuged at 300 × g, then at 1000 × g, and finally at 100 000 × g to remove any debris (the supernatant was transferred to a new tube between each centrifugation). Aliquots (5 mL) from the spent medium of each RPE cell culture were taken and concentrated 100 times under vacuum centrifugation. The samples were then desalted against 10 mM Tris HCl, pH 7, using P6 Bio-Spin columns (Bio-Rad, Hercules, CA) and the protein content was determined using the Bio-Rad protein assay reagent following the manufacturer's instructions (Bio-Rad, Hercules, CA). Equal aliquots of labeled and un-

labeled RPE secreted proteins were mixed together and then separated by SDS-PAGE. Coomassie-stained protein bands were digested with a gold grade trypsin (Promega, Madison, WI) and the resulting peptide solutions were passed through a 0.2 μm PVDF filter (0.22 μm pore size) prior to LC−MS/MS analysis.

Nanoflow LC−MS/MS. Nano-LC tandem mass spectrometry was performed on an LC−Packing system (DIONEX UltiMate Capillary/Nano LC System, Dionex Corp., Sunnyvale, CA) connected to a Linear Ion Trap (LTQ) mass spectrometer (Thermo Electron Corporation, San Jose, CA). Each sample was injected via an autosampler and loaded onto a C18 trap column (300 μm × 1 mm, LC Packings) for 6 min at a flow rate of 10 μL/min. The sample was subsequently separated by a C18 reverse-phase column (75 μm × 15 cm, Vydac, Columbia, Maryland) at a flow rate of 300 nL/min. The mobile phases consisted of water with 0.1% formic acid (A) and 90% acetonitrile with 0.1% formic acid (B). A 90-min linear gradient from 5 to 50% B was typically employed. After LC separation, the sample was introduced into the mass spectrometer via a 10-μm silica tip (New Objective Inc., Ringoes, NJ) adapted to a nano-electrospray source (Thermo Electron Corporation, San Jose, CA). The spray voltage was set at 2.0 kV and the heated capillary at 160 °C. The LTQ was operated in data-dependent mode in which one cycle of experiments consisted of one full-MS survey and subsequently three sequential pairs of intercalated zoom scans and MS/MS experiments. The targeted ion counts in the ion trap during full-MS, zoom scan, and MS/MS were 30 000, 3000, and 10 000, respectively. The zoom scan events are of higher resolution and were used to determine the charge state of the ion as well as the ratio of labeled and unlabeled peptide pairs using the ZoomQuant software (see next section). Peptides were fragmented in the linear ion trap using collision-induced dissociation with the collision gas (helium) pressure set at 1.3 milliTorrs and the normalized collision energy value set at 35%.

Database Search. Protein searches were performed with the BioWorks 3.2 software (Thermo Electron Corp, San Jose, CA). Basically, each file was searched against the human NCBInr and the human SwissProt databases using the Sequest search engine set with the following possible protein modifications: 16 Da shift for oxidized Met and 6 and 8 Da shifts for stable isotope labeled Arg and Lys, respectively. The acceptance criteria for peptide identifications were set as follows: a DeltaCn (ΔCn) > 0.1, a variable threshold of *Xcorr* vs charge state (*Xcorr* = 1.9 for $z = 1$, *Xcorr* = 2.5 for $z = 2$, and *Xcorr* = 3.5 for $z \geq 3$) and a peptide probability based score with a p value < 0.001. The rate of false positive identification was determined (using the same filtration criteria) by searching the files against a reversed human NCBInr database. Using these stringent filtration criteria, the rate of false positive identification was less than 1.8%, thus increasing the confidence in the identified proteins.

ZoomQuant Analysis. To measure the intensity ratios of labeled and unlabeled peptide pairs, we used the ZoomQuant software developed by Halligan et al.[34] The generated Sequest output files were loaded into the Epitomize filter to generate a colon-delimited text file that contained the list of identified proteins, the sequence and atomic composition of the identified peptides with scan number, charge state, *Xcorr*, and mass data. This file was then loaded into the ZoomQuant software along with a file containing zoom scans that were extracted from the corresponding raw data file using a visual basic RawBitz script. Zoom scan information was then matched to the Sequest identified peptides, after which labeled and unlabeled pairs were detected based on their amino acid composition and theoretical masses. Ratios were determined from the peak areas of the isotope clusters of the labeled and unlabeled peptides.

mRNA Isolation and Expression Profiling. Total RNA was isolated from several RPE cell cultures: healthy donors with the wild-type CFH genotype ($n = 4$), AMD donors with homozygous rare Y402H−CFH genotype ($n = 3$), and AMD donors with heterozygous Y420H−CFH genotype ($n = 3$) using TRIZOL reagent (Invitrogen, Carlsbad CA) and then cleaned up using a Qiagen Kit according to the manufacturer's protocol. Total RNA was then converted to double biotinylated cRNAs and hybridized to separate Affymetrix Human U133 Plus 2.0 GeneChips. Procedures for cRNA preparation and GeneChip processing were performed as previously described.[35,36]

Ingenuity Pathway Analysis. Differentially expressed proteins were evaluated by the Ingenuity computational pathway analysis software to identify possible global functions of the secreted protein pattern and association with the disease. The Ingenuity Pathway Analysis program uses a knowledge base derived from the literature to relate gene products to each other, based on their interaction and function. The knowledge base consists of a high quality expert-curated database containing 1.4 million biological findings consisting of more than 23 900 mammalian genes (10 300 for human, 5200 for rat, and 8400 for mouse) and millions of pathway interactions extracted from the literature. This knowledge database also integrates a broad range of systems biology including protein function, cellular localization, and small molecule and disease interrelationships. The Ingenuity Pathway Analysis suite identifies dynamically generated biological networks, global canonical pathways, and global functions. Basically, the relevant proteins with their fold change and corresponding "gi" accession number are uploaded as an Excel spreadsheet file into the Ingenuity software (http://www.ingenuity.com). Ingenuity then uses these proteins and their identifiers to navigate the curated literature database and extract an overlapping network between the candidate proteins. A score better than 2 is usually attributed to a valid network (the score represents the log probability that this network was found by random chance).

Results

Electron Microscopy Examination of Macular Biopsies. Examination of sections of the macula using electron microscopy is an effective way to determine and classify different histological AMD features.[37] Figure 1 shows a cross section of the macula from the eyes of 81 year old (A), 72 year old (B), and 77 year old (C) donors. The cross section of the retina is represented by three well-defined areas, namely the RPE, Bruch's membrane and the choroids (Figure 1A). Both the 72 year-old donor (Figure 1B) and the 77 year old donor (Figure 1C) retinal cross sections presented with deposits just beneath the basal lamina of the RPE whereas the retinal cross section of the 81 year-old donor appears free from deposits with the RPE cells perfectly aligned atop of Bruch's membrane (Figure 1A). The basal laminar deposits called fibrous long-spacing collagen (FLSC) seen in the retinal section from the 72 year-old donor (Figure 1B) are accompanied by a thickening of Bruch's membrane which is believed to be consistent with the early stages of AMD.[37] An increase in the number and volume of these deposits is highly indicative of progressive AMD.

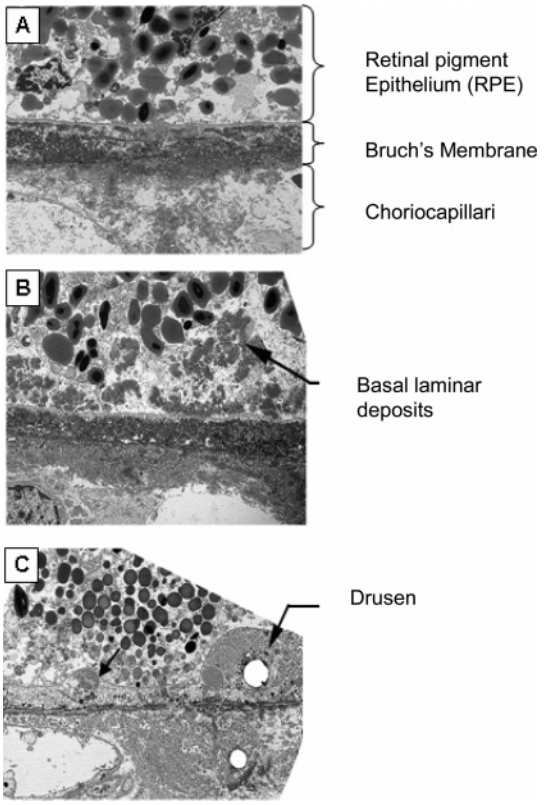

Figure 1. Electron micrographs of the cross section of the macula prepared from an (A) 81-, (B) 72-, and (C) 77-year old donor. The black arrow indicates the "fibrous long-spacing collagen" between the RPE and Bruch's membrane seen in donor (B) and drusen particles seen in donor (C).

RPE cells were isolated from the retina of these autopsied eyes and resulted in growing colonies that could be propagated up to passage 12 before entering into a senescence phase. Thirty-five primary RPE cultures of 27 human subjects (RPE cultures were obtained from both the left and right eye of some subjects) were generated. Cultures were examined for their epithelial cell content using FACS analysis.[24] Only cell cultures with high epithelial content (equal to or greater than 80%) were kept for the study.

RPE Genotyping for the CFH Variant. Each of the RPE cell cultures generated from AMD patients and normal donors were genotyped for the AMD-predisposing SNP (Y402H−CFH)[8−11] as described in the experimental methods. RPE cell cultures generated from the left and right eye of the same donor had the same genotype demonstrating the validity of our assay. Among the 35 genotyped RPE cell cultures, 14 were wild type (TT), 16 were heterozygote (CT), and only 5 harbored the homozygote rare CFH genotype (CC) associated with AMD. The EM histological examination did not always correlate with the CFH genotyping especially in the wild-type and heterozygous samples. Indeed, among the 14 RPE cell cultures with the wild-type CFH genotype (TT-RPE), we were able to diagnose 5 with healthy macula (absence of any kind of deposit), 2 with basal laminar deposits (early stage AMD), and 3 with drusen deposits, whereas the rest (4 RPE cultures) had inconclusive diagnoses. Among the 16 RPE cell cultures with the heterozygous CFH genotype (CT-REP) we were able to obtain conclusive diagnoses for 7 samples (3 with healthy macula, 2 with early stage AMD and 2 with large drusen deposits). Finally, 3 out of the 5 RPE cell cultures with the homozygous rare CFH genotype had large drusen deposits whereas 2 had completely healthy macula. These results are not surprising because not all individuals with clinically documented AMD have the CFH gene variant and conversely, not all individuals free of AMD are wild type at this locus. Similar findings were reported by Hageman et al.[11] in a study performed on a cohort of AMD cases ($n = 404$) and age-matched controls ($n = 131$). Among the 404 AMD cases, only 146 were found to harbor the CC homozygous variant whereas 183 harbored the heterozygous CT variant and 74 displayed the TT wild-type genotype. Among the 131 control cases, 16 were found to harbor the homozygous CC genotype, 56 the heterozygous CT genotype, and 59 the TT wild-type genotype. These results suggest that AMD may be the result of more complex genetic factors acting in concert with environmental risk factors. Indeed, a recent genotyping study performed on a large cohort of AMD and control cases demonstrated that, aside from the complement factor H variant, there are additional SNPs that can protect or worsen one's risk of developing AMD.[12] Classification of any predisposing alleles may help define an individual's risk for AMD, whereas understanding the cellular and molecular mechanisms of the pathology (e.g., drusen formation and angiogenesis) may aid in defining therapeutic targets. In this study, we hypothesize that proteins secreted by the RPE are involved in drusen formation.

Analysis of RPE Secreted Proteins. The advantage of growing RPE cells in stable isotope labeled amino acid containing medium is that all cellular proteins are uniformly labeled with heavy isotope amino acids (e.g., $^{13}C_6$−Arg and $^{13}C_6$, $^{15}N_2$−Lys), making it easy to distinguish RPE secreted proteins from bovine serum contaminants. Indeed, several bovine proteins were still present in the culture medium even after washing the cells five times with PBS before incubating them in a serum-free conditioned medium (Figure 2b). Additionally, bovine serum proteins may be erroneously identified as their human homologues even after restricting protein database searches to human NCBInr fasta, thereby raising doubts as to the true origin of the identified protein. This problem was easily circumvented by using SILAC and by selecting only those proteins represented by labeled and unlabeled peptide pairs for further analysis (Figure 2c). The detection of these peptide pairs was performed automatically by ZoomQuant software.[34] Basically, the software uses the peptide sequences generated by a Sequest database search, then calculates the theoretical mass of the peptide and looks for labeled and unlabeled peptide pairs based on Arg and Lys residue content. This procedure permits all single peptides generated from bovine proteins and/or other contaminants such as keratins to be filtered out. Only proteins represented by labeled and unlabeled peptide pairs are retained. Table 1 summarizes all the 72 proteins we have identified thus far in mixtures of spent media from labeled and unlabeled RPE cell cultures. Most of the reported peptides were identified with *X-corr* scores above 2.5 and 3.5, for the doubly and triply charged ions, respectively and a p value < 0.001 for peptide probability based score. The rate of false positive identification was less than 1.8% when a database search was performed against reversed fasta formats of human NCBInr and human SwissProt databases using the same filtration criteria. Although 13 out of the 72 proteins were represented by a single peptide, it was still possible to confidently identify these proteins based on the fact that both labeled and unlabeled peptide were detected and also by manually checking the corresponding MS/MS spectrum. Labeled and unlabeled peptide pairs readily validate each other,

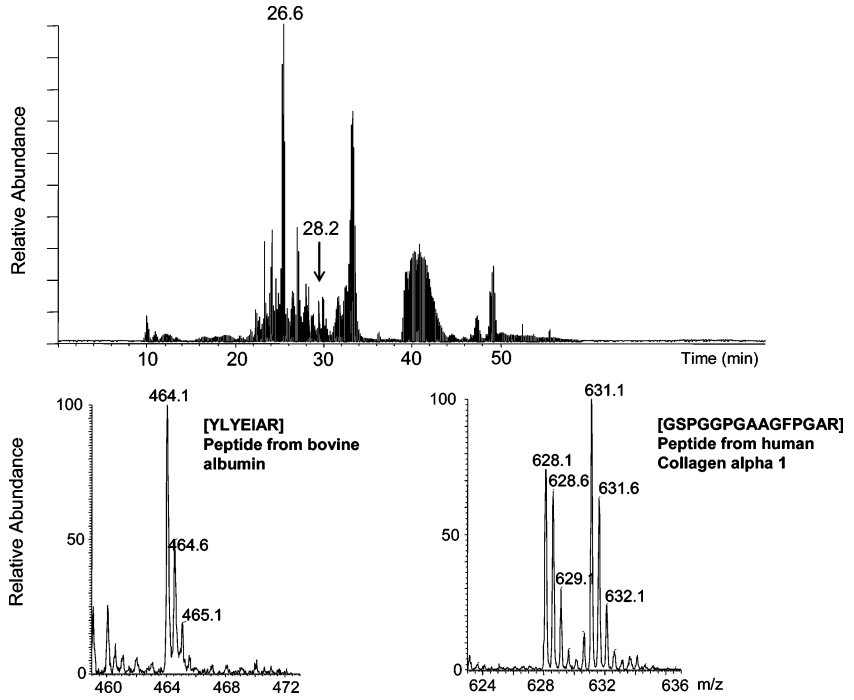

Figure 2. LC−MS run of peptides generated by tryptic in-gel digestion of a gel slice obtained from an SDS-PAGE run of a 1:1 mixture of labeled and unlabeled RPE secreted proteins. The top graph is the base peak chromatogram showing the overall peak intensities and retention time of all the peptides detected in this gel slice. The bottom shows the zoom scan mass of two consecutive eluting peptides. The peptide with *m*/*z* 461 eluting at 26.6 min was detected as a singlet and belongs to bovine serum albumin as well as human albumin. The peptide eluting at 28.2 min was detected as a doublet peak at *m*/*z* 628.1 and 631.1, corresponding to the unlabeled and labeled peptide, respectively. This belongs to human RPE cells. Peptide sequences are shown on the top of each spectrum and were obtained by MS/MS analysis and database search. The labeled and unlabeled peptides are 6 Da apart and agree with one $^{13}C_6$−Arg residue in the peptide sequence.

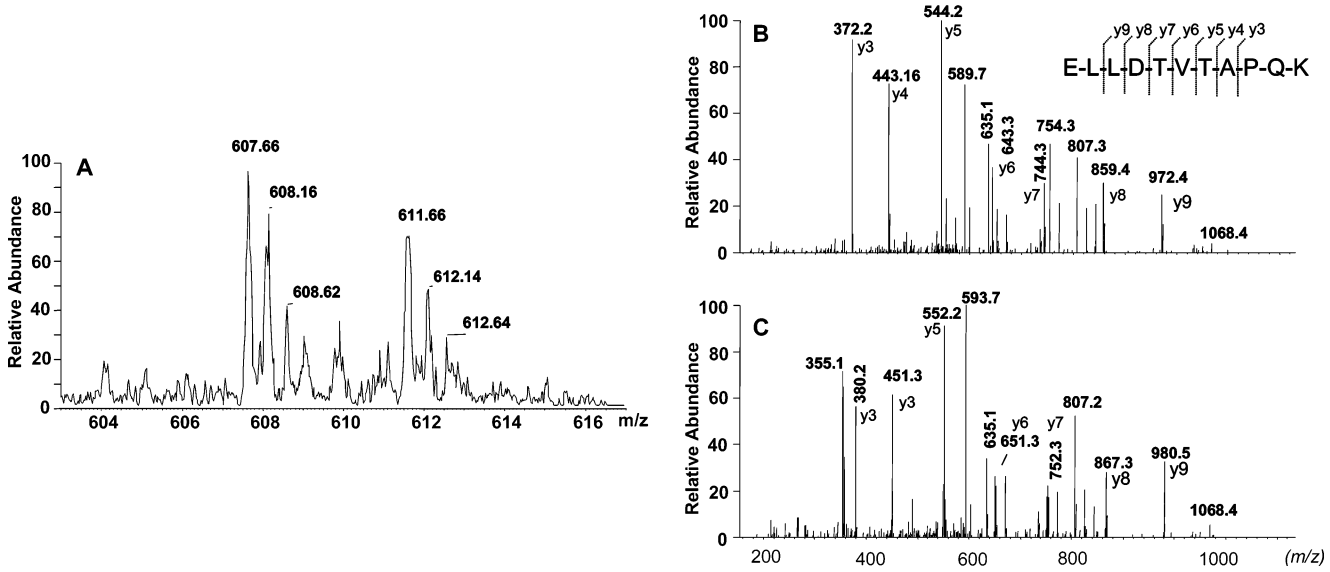

Figure 3. LTQ MS and MS/MS spectra of labeled and unlabeled peptide pairs detected for PEDF in a 1:1 mixture of spent media of unlabeled and $^{13}C_6$−Arg, $^{13}C_6$, $^{15}N_2$−Lys fully labeled RPE cells. (A) Top spectrum shows the zoom scan MS of labeled and unlabeled peptide pairs (*m*/*z* 607.66 and 611.66). These peaks correspond to a doubly charged ion species. Because the difference in *m*/*z* between labeled and unlabeled peptides is 4, this suggests that the peptide should contain a K (Lys) residue. (B) Bottom spectrum shows MS/MS of both unlabeled peptide at *m*/*z* 607.66 and labeled peptide at *m*/*z* 611.66. The series of y ions are all shifted by 8 Da in the labeled versus unlabeled peptide, confirming the peptide sequence [ELLDTVTAPQK] for human PEDF.

thus adding more confidence in the identification of these proteins. Figure 3a represents the mass spectrum obtained for pigment epithelium derived factor protein (PEDF) with peaks for unlabeled and labeled peptide pairs at *m*/*z* 607.66 and 611.66, respectively. The difference in mass between these doubly charged ions is 8 Da, suggesting that the peptide should contain one Lys residue (i.e., $^{13}C_6$, $^{15}N_2$−Lys). This was further confirmed by the MS/MS analysis of both labeled and unla-

Table 1. List of Proteins Identified in the Spent Media of Human Primary RPE Cell Cultures

protein name	accession number	peptide counts	secreted
Cell adhesion/connective tissue protein			
47 kDa heat shock protein precursor	123576	1	YES
alpha 1 type I collagen preproprotein	22328092	1	YES
alpha 2 type VI collagen isoform 2C2a precursor	17402879	2	YES
alpha 2(I) collagen	2388555	3	YES
basement membrane-specific heparin sulfate	24212664	6	YES
BIGH3	2996636	1	YES
biglycan preproprotein	4502403	4	YES
collagen alpha 1(I) precursor	115269	40	YES
collagen alpha 1(III) precursor	4502951	35	YES
collagen alpha 2(I) chain precursor	82654930	29	YES
collagen, type VI alpha 1 (VI) chain precursor	13878903	10	YES
fibulin-1 precursor	30581038	7	YES
galectin 3 binding protein	5031863	9	YES
fibronectin 1	34364820	49	YES
immunoglobulin superfamily containing leucine	5031809	1	YES
laminin, alpha 4 precursor	4504949	8	YES
laminin, beta 1 precursor	4504951	10	YES
laminin gamma-1 chain precursor	126369	11	YES
migration stimulation factor	27227743	8	YES
thrombospondin 1 precursor	40317626	6	YES
thrombospondin 2 precursor	549136	4	YES
Complement regulator/immune response			
clusterin precursor	116533	5	YES
complement C1r component precursor	115204	4	YES
complement C1s	6407558	3	YES
complement C4-B	81175167	3	YES
complement component 1 inhibitor precursor	15029894	7	YES
complement factor B precursor	584908	4	YES
complement factor H precursor	85681919	3	YES
neuroleukin	189238	4	NO
pentaxin- related gene	4506333	4	YES
Protease/protease inhibitor			
carboxypeptidase A4	61743916	11	YES
caspase 5	4757914	1	NO
glia-derived nexin precursor	183064	6	YES
matrix metalloproteinase 2 preproprotein	11342666	2	YES
plasminogen activator inhibitor type 1	24307907	8	YES
procollagen C-endopeptidase enhancer	4505643	2	YES
the Mmp-inhibitory	6730224	2	YES
Catabolism			
aldolase A	229674	5	NO
alpha enolase	2661039	13	YES
protein disulfide-isomerase	2135267	3	YES
similar to triosephosphate isomerase 1	16877874	6	NO
transketolase	4507521	1	NO
Cell organization and biogenesis			
ACTN4 protein	33874637	7	NO
ezrin	119717	2	NO
gelsolin isoform a	4504165	4	YES
insulin-like growth factor binding protein 3	62243068	1	YES
insulin-like growth factor binding protein 7	4504619	3	YES
quiescin Q6	13325075	5	YES
TUBA6 protein	21619816	1	NO
Development			
annexin 5	4502107	1	NO
decorin isoform a preproprotein	4503271	2	YES
decorin isoform b precursor	19743848	2	YES
glutathione tranferase	4504183	2	NO
pigment epithelium-derived factor	1144299	10	YES
secreted protein, acidic, cysteine-rich	4507171	7	YES
Other functions			
14−3−3 gamma protein	5726310	2	NO
alpha actinin	28723	11	NO
alpha-fetoprotein precursor	4501989	3	YES
beta-trace	410564	1	NO
CALU	49456627	12	YES
extracellular matrix protein 1 isoform 1 precursor	4758236	2	YES
follistatin-like 1 precursor	5901956	3	YES
lumican	4505047	8	YES
moesin/anaplastin lymphoma kinase fusion protein	14625824	2	NO

Table 1. (Continued)

protein name	accession number	peptide counts	secreted
mutant beta-actin	28336	8	NO
nucleobindin 1 precursor	2506255	1	YES
phosphoglycerate mutase processed protein	20530939	3	NO
phosphopyruvate hydratase (Beta-enolase)	105934	3	NO
muscle specific enolase	31167	3	NO
PRO1708	7959791	1	NO
prostaglandin D2 synthase	32171249	2	YES
tarsh protein	33667044	4	YES
tyrosine 3-monooxygenase	30584583	1	NO

Table 2. Differential Expression of Some Secreted Proteins in the RPE Cells of AMD and Age-Matched Healthy Control Donors

protein name	accession number	secretion	ratio (scan numbers)[a] TT/TT	CT/TT	CC/TT
Cell adhesion/connective tissue protein					
collagen alpha 1(I) precursor	115269	YES	1.51 ± 0.23 (09)	1.20 ± 0.37 (04)	1.56 ± 0.15 (06)
collagen alpha 1(III) precursor	4502951	YES	0.98 ± 0.15 (22)	0.84 ± 0.08 (10)	1.51 ± 0.23 (27)
collagen alpha 2(I) precursor	82654930	YES	1.53 ± 0.30 (10)	1.21 ± 0.10 (03)	1.71 ± 0.17 (16)
galectin 3 binding protein	5031863	YES	1.05 ± 0.02 (02)	1.63 ± 0.15 (03)	2.22 ± 0.27 (11)
fibronectin 1	34364820	YES	1.39 ± 0.17 (16)	2.02 ± 0.23 (13)	2.72 ± 0.35 (16)
lumican	4505047	YES	1. 58 ± 0.00 (01)	ND	3.45 ± 0.55 (04)
migration stimulation factor	27227743	YES	1.36 ± 0.00 (01)	2.10 ± 0.09 (03)	2.71 ± 0.26 (05)
Complement regulator/immune response					
clusterin precursor	116533	YES	0.92 ± 0.00 (01)	2.34 ± 0.30 (03)	3.23 ± 0.28 (02)
complement C1r component precursor	115204	YES	ND	1.79 ± 0.00 (01)	2.20 ± 0.12 (02)
complement C1s	6407558	YES	ND	1.61 ± 0.00 (01)	1.99 ± 0.27 (02)
complement component 1 inhibitor precursor	15029894	YES	0.92 ± 0.00 (01)	1.54 ± 0.17 (02)	1.60 ± 0.20 (06)
complement factor B precursor	584908	YES	ND	1.14 ± 0.00 (01)	1.54 ± 0.00 (01)
complement factor H precursor	85681919	YES	2.16 ± 0.00 (01)	1.84 ± 0.38 (02)	3.29 ± 0.02 (02)
Protease/protease inhibitor					
carboxypeptidase A4	61743916	YES	1.33 ± 0.00 (01)	0.98 ± 0.00 (01)	1.76 ± 0.31 (06)
matrix metalloproteinase 2	11342666	YES	1.49 ± 0.00 (01)	ND	3.39 ± 0.47 (03)
tissue inhibitor of metalloproteinase-1	6730224	YES	1.05 ± 0.18 (02)	1.25 ± 0.04 (02)	2.37 ± 0.12 (03)
Development					
pigment epithelium-derived factor	1144299	YES	1.36 ± 0.00 (01)	2.14 ± 0.00 (01)	2.75 ± 0.10 (03)
secreted protein, acidic, cysteine-rich (osteonectin)	4507171	YES	1.23 ± 0.06 (02)	0.59 ± 0.14 (02)	0.58 ± 0.04 (02)
Other functions					
extracellular matrix protein 1 isoform 1 precursor	4758236	YES	ND	2.77 ± 0.00 (01)	ND

[a] Ratios were determined between labeled and unlabeled peptide pairs and the standard deviation was obtained based on the number of detected peptides per protein; these are included between parentheses. ND: not determined; TT: RPE cells from healthy control donors with the wild-type CFH genotype; CT: RPE cells from AMD donors with the heterozygous Y402H−CFH genotype; CC: RPE cells from AMD donors with the homozygous rare Y402H−CFH genotype.

beled peptides (Figures 3b and 3c). Peaks representing the "y" ion series were all shifted by 8 Da in the MS/MS spectrum of the labeled peptide (Figure 3c) versus those of the unlabeled peptide (Figure 3b), whereas the "b" ion series remained unchanged.

Secreted Protein Profiling in RPE Cells Prepared from AMD and Normal Age-Matched Healthy Donors. To measure secreted protein levels in RPE cells from AMD versus normal donors, we analyzed 1:1 protein mixtures of spent media from fully labeled TT-RPE (wild-type control) cell cultures and from each of the unlabeled CT-RPE or CC-RPE cell cultures prepared from AMD donors with the homozygous rare and heterozygous Y402H−CFH genotypes, respectively. A control unlabeled TT-RPE was prepared from a different control donor and compared to the labeled TT-RPE. Because of the sequence homology between some human and bovine proteins, only peptide sequences unique to human proteins were used to determine protein ratios. Figure 4 shows an example for PEDF protein (87.5% sequence homology between human and bovine) where the ratio between labeled and unlabeled peptides is skewed when the same peptide sequence is shared between human and bovine proteins. Although the cells were carefully washed with PBS before incubation in serum-free media, there were still some bovine proteins present in the spent media. Because it is not possible to control the level of bovine protein contamination between samples, we decided to use only peptide sequences that are unique to human proteins for further analysis. Labeled and unlabeled peptide pairs unique to human proteins were thus detected, and their ratios were measured using ZoomQuant software. The ZoomQuant script, which was previously designed to quantify peptide ratios generated from an ^{18}O proteolytic experiment,[34] was slightly modified in the present study to accommodate data generated from a SILAC experiment using $^{13}C_6$−Arg and $^{13}C_6$, $^{15}N_2$−Lys as the labeling amino acids. Table 2 summarizes some of the secreted proteins for which ratios between normal and AMD RPE cells were obtained. In general, these ratios were close to 1 (mean average ratio = 1.26 ± 0.3) for most of the proteins when labeled TT-RPE cells (healthy control) were compared to unlabeled TT-RPE cells prepared from another healthy control donor. However, some of these same proteins were found differentially expressed when RPE cells of healthy

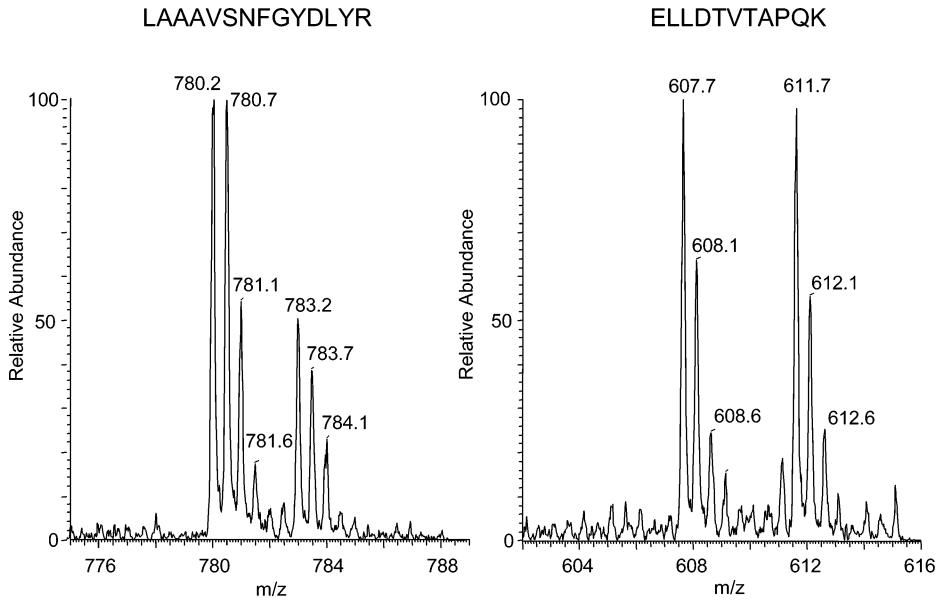

Figure 4. Zoom MS scans of two peptides for PEDF. The peptide on the left (LAAAVSNFGYDLYR) was found in both bovine and human PEDF whereas the peptide on the right (ELLDTVTAPQK) was unique to human PEDF. The ratio of the intensity of labeled to unlabeled peptides was decreased for the peptide in the left due the remaining bovine unlabeled PEDF present in the RPE spent medium.

controls with the wild-type genotype (TT-RPE) were compared to RPE cells of AMD donors with the heterozygous (CT-RPE) or homozygous rare (CC-RPE) Y402H−CFH genotype. Overall, CT-RPE and CC-RPE secreted at least 2-fold more clusterin, fibronectin, galectin 3 binding protein, lumican, PEDF, matrix metalloproteinase 2 (MMP2), tissue inhibitor for metalloproteinase-1 (TIMP-1), and complements C1r and C1s than the TT-RPE cells prepared from age-matched healthy donors. SPARC was found to be down regulated by almost 2-fold in AMD RPE cells when compared to healthy RPE cells. We used 1.6 as a significant cut off for fold change based on the mean average value obtained between two RPE cell cultures derived from two healthy donors (mean average ratio = 1.26 ± 0.3).

We further analyzed mRNA expression levels of this same set of differentially expressed proteins using a larger sample size of RPE cell cultures prepared from AMD donors with the homozygous rare ($n = 3$) and the heterozygous ($n = 3$) Y402H−CFH genotype and from age-matched healthy donors ($n = 4$). The mRNA level for all the selected proteins remained unchanged between AMD RPE cells (CT-RPE and CC-RPE) and healthy TT-RPE cells except for clusterin, whose mRNA levels seem to reflect the trend observed at the protein level (Figure 5). The general poor correlation between mRNA and protein levels was previously reported in several systems[38−40] and might be due to differences in half-lives between mRNA and proteins.

Network Analysis. To analyze the overlapping network function between all the secreted proteins whose levels were found altered in AMD RPE cells versus normal RPE cells, we uploaded the set of proteins from Table 2 with their accession numbers and expression levels into the Ingenuity pathway analysis software. An overlapping network with a score of 35 (i.e., score > 2 is significant; it represents the log of the probability that the overlapping network was found by random chance) was obtained for 16 of the 19 uploaded proteins (Figure 6). Among the 19 uploaded proteins, 17 are known to be extracellular proteins whereas 2 (fibronectin and galectin 3 binding protein) are plasma membrane surface proteins, though these two proteins are also noted as secreted proteins in the SwissProt database. Upon examination, the most relevant

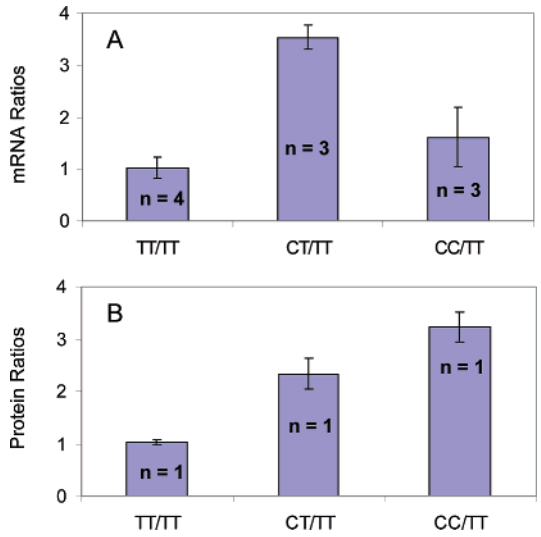

Figure 5. mRNA and protein ratio profiles for clusterin in different RPE cell cultures prepared from AMD donors with the homozygous rare (CC) and heterozygous (CT) Y402−CFH genotype versus RPE cells prepared from age-matched healthy donors with the wild-type CFH genotype (TT). The ratios are all normalized to a healthy RPE culture with the wild-type CFH genotype (TT). The top graph is for mRNA profiling and the measurements represent the average values obtained for 4 TT-RPE, 3 CT-RPE, and 3 CC-RPE cultures. The bottom graph is for ratios obtained at the protein level between pairwise comparisons of a CT-RPE, CC-RPE, and TT-RPE culture to another TT-RPE culture.

function extracted from this overlapping network was related to tissue development and angiogenesis and included 9 proteins out of the 19 uploaded. Fibronectin, MMP2, PEDF, and SPARC were all found to be involved in the remodeling of the extracellular matrix as well as regulating angiogenesis. Other proteins such as clusterin, complement factor B, CFH, and complement C1r and C1s are involved in immunological as well as inflammatory diseases, whereas lumican, galectin 3 binding protein, and fibronectin proteins were found to be involved in

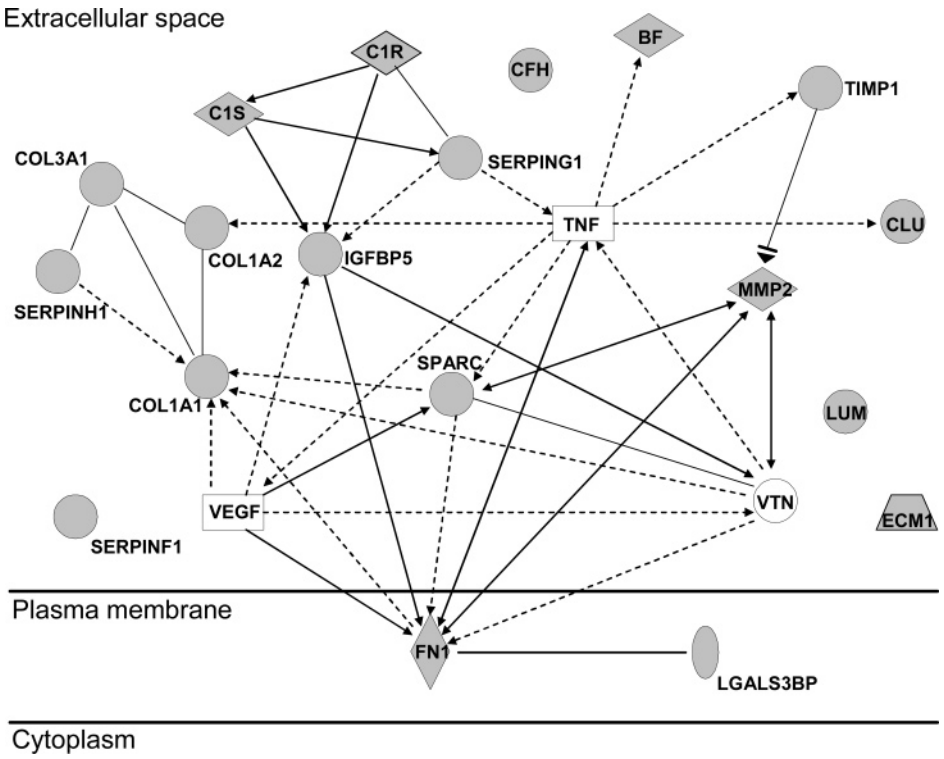

Figure 6. Ingenuity pathway network obtained on a set of differentially secreted proteins detected in RPE cells derived from an AMD donor (with macular deposits and the homozygous rare Y402H−CFH genotype) versus RPE cells derived from an age-matched healthy donor (see data from Table 2). Proteins with their gi number and corresponding fold change between the two cell cultures were uploaded into Ingenuity pathway analysis software (http://www.ingenuity.com). Proteins with a gray background were detected in the RPE spent media while other interacting proteins with a clear background were not detected in the spent media. BF: Complement Factor B, C1R: Complement C1r component precursor, C1S: Complement C1s, CFH: Complement Factor H, CLU: Clusterin, COL1A1: Collagen alpha 1(I) precursor, COL1A2: Collagen alpha 2(I) precursor, COL3A1: Collagen alpha 1(III) precursor, ECM1: Extracellular matrix protein 1 isoform 1 precursor, FN1: Hypothetical protein (Fibronectin 1), IGFBP5: Insulin-like growth factor binding protein 5, LGALS3BP: Galectin 3 binding protein, LUM: Lumican, MMP2: Matrix metalloproteinase 2 preproprotein, SERPINF1: Pigment epithelium-derived factor, SERPING1: Complement component 1 inhibitor precursor, SERPINH1: heat shock protein 47, SPARC: Secreted protein, acidic, cysteine-rich, TIMP1: The Mmp-inhibitory, TNF: Tumor Necrosis Factor, VEGF: Vascular Endothelial Growth Factor, VTN: Vitronectin. The major interactions found between these proteins are indicated by different arrows.

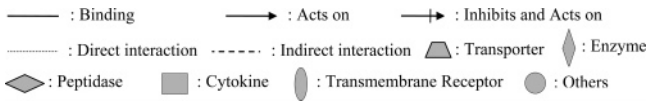

cell adhesion and cellular matrix build up. Most of these secreted proteins were found to directly interact with each other such as MMP2 and its inhibitor TIMP. Thus, the balance in the relative quantities of these proteins in the extracellular space might be crucial for maintaining tissue homeostasis at the interface between RPE and Bruch's membrane.

Discussion

It has long been hypothesized that RPE cells might be involved in the biogenesis and formation of drusen,[13] however only few studies have actually examined the direct relationship between RPE cells and drusen formation,[41−43] using RTPCR or immunostaining for the relevant proteins. In the present study, we investigated secreted proteins, the "secretome", of RPE cells using a SILAC-based strategy and examined their levels in AMD versus normal cells. In general, RPE cells were found to secrete a variety of connective tissue proteins, extracellular matrix proteins, complement factors, proteases, as well as protease inhibitors. Among the 72 proteins detected in the spent media, 53 were found to have a signal peptide for secretion according to the Swiss-Prot/TrEMBL database and/or by using the SignalP 3.0 predictor software (http://www.cbs.dtu.dk/services/SignalP). The remaining 19 proteins corresponded to nonsecreted proteins, and this could have been the result of protein leakage or exocytosis vesicles in the spent media. Most importantly, some of the secreted proteins such as fibronectin, clusterin, complement factors, TIMP, and annexins are major components of drusen,[11,44,45] and these were readily secreted by RPE cells. These findings clearly support the overall hypothesis that RPE cells might be directly involved in drusen formation. To our knowledge, this is the first evidence that RPE cells make and secrete their own CFH, the protein containing the Y402H variant that is strongly associated with the risk of developing AMD.[8−11] This local secretion of CFH by RPE cells could be highly relevant to AMD pathology. Indeed, CFH plays a critical role in protecting cells from complement attack as well as decreasing and limiting immune complex deposition as demonstrated in glomeruli of CFH-deficient mice,[46] which develop a renal disease that clinically resembles AMD. We hypothesize that the Y402H−CFH variant synthesized by RPE cells from

AMD donors is dysfunctional and unable to efficiently clear the debris that accumulates between the basal lamina of RPE cells and Bruch's membrane to form drusen deposits. Unfortunately, because of the low abundance of this protein in the spent media, only 3 peptides were detected in this study, which did not allow for us to analyze whether the protein was mutated at position 402 in the RPE cells prepared from AMD donors with the homozygous Y402CFH genotype. Further investigation using more samples is needed to obtain better sequence coverage for this protein and to determine its primary structure and potential activity.

The elevated secretion of clusterin seen in AMD versus normal RPE cells was significant both at the mRNA and protein levels. The exact function of clusterin is not well understood, but it is implicated in several functions such as response to cellular injury, lipid transport, apoptosis, and clearance of cellular debris caused by cell injury or death.[47] Recent reports show that clusterin is a major constituent of drusen collected from AMD donors and could be directly involved in their formation.[44,48] This protein was described to have a promiscuous binding property thus, it has been suggested that its accumulation at the RPE-Bruch's membrane inter-space could attract a myriad of molecules resulting in a nucleation site for drusen biogenesis.[48] More interestingly, clusterin was found to promote amyloid plaque formation in a mouse model of Alzheimer's disease[49] and drusen-like Alzheimer's aggregates do contain a large amount of β-amyloids,[50,51] thus the elevated secretion of clusterin seen in the AMD donors could be directly involved in drusen biogenesis. Another interesting hypothesis that could directly link clusterin to immune complex mediated drusen formation is that clusterin functions as a complement regulatory protein.[52] The increased secretion of clusterin by RPE cells of AMD donors could be a compensatory effect to correct for the low activity of the Y402H−CFH rare variant protein and this may result in even more debris accumulation given that clusterin attracts a variety of proteins. Overall, AMD RPE cells secreted more complement and complement factors than healthy RPE cells and this is in agreement with the large amount of complement detected in drusen.[11]

Conversely, the 3-fold increase in MMP-2 secretion seen in AMD RPE cells versus healthy RPE cells correlates with previous studies which showed that RPE- associated interphoto receptor matrices collected from AMD donor eyes contained 2-fold more MMP-2 than those collected from age-matched healthy control donor eyes.[53] Despite the fact that MMPs are not detected in drusen,[54] their role in AMD pathology might reside in their indirect involvement in angiogenesis via their proteolytic activity and remodeling of the extracellular matrix.[55] Indeed, using a knockout mouse model, it has been shown that MMP-2 and MMP-9 deficient mice were more protected against laser-induced CNV than wild-type mice expressing MMPs.[55] Thus, increased secretion of MMPs in the RPE cells of AMD donors could contribute to the risk of developing CNV. Nevertheless, this protein is tightly controlled by TIMP, which also showed a 2-fold increase in expression in AMD RPE cells versus healthy RPE cells. The ratio between MMP and TIMP might be involved in the regulation of angiogenesis. Unfortunately, we were not able to detect all isoforms of MMPs and their corresponding TIMPs to establish this overall balance in the spent media of AMD RPE cells versus healthy RPE cells. Angiogenesis is a complex tissue development event and involves several regulatory factors that need to be comprehensively measured and tested.

SPARC is another protein found in the spent media of RPE cells and might also be involved in angiogenesis. Because of the high homology found between human and bovine SPARC protein (i.e., 98.7% sequence homology) we could not detect any peptides that were unique to human SPARC to obtain more accurate protein ratios. Thus, all detected peptides for SPARC were used as an average to estimate the ratio for this protein across all samples (only peptides that were consistently detected across all the samples were used to estimate this ratio). Overall SPARC protein expression was found to be down regulated in AMD RPE cells versus healthy RPE cells by ~2-fold. SPARC, also known as osteonectin, has anti-adhesive properties and was recently reported to play a key role in the regulation of attachment-detachment of the RPE monolayer to Bruch's membrane.[56] Importantly, the decreased expression of SPARC in AMD donors could favor angiogenesis as this protein was found to have a potent inhibitory effect on angiogenesis.[57,58] Additionally, SPARC can also stimulate angiogenesis after proteolytic cleavage by MMPs.[59,60] Thus, the 3-fold increase in expression of MMP-2 in RPE cells of AMD versus healthy donors would favor angiogenesis by decreasing the amount of SPARC in the extracellular space while producing potent angiogenic SPARC peptides. This could explain the protective effect against laser-induced CNV seen in MMP-2 and MMP-9 deficient mice.[55]

PEDF is another potent inhibitor of angiogenesis in the mammalian ocular compartment.[61] Surprisingly, the RPE prepared from AMD donors secreted more PEDF than the RPE from healthy controls. A slight increase was also observed at the mRNA level for RPE cells prepared from AMD donors with heterozygous CFH genotype ($n = 3$) versus RPE cells prepared from age-matched healthy controls ($n = 4$) (data not shown). This intriguing increase of PEDF secretion (inhibitor of angiogenesis) in AMD cells was also reported by others in CNV-derived RPE cells[62] and could be the result of a compensatory effect to outbalance the angiogenic activity of VEGF, which might be present in the retinal extracellular environment. Indeed, angiogenesis is tightly controlled by the balance between PEDF and VEGF.[63] Unfortunately, we did not detect VEGF in this study and thus we could not determine the ratio between PEDF and VEGF. More specific experimental approaches might be needed to assess the overall amount of angiogenesis regulating factors in the spent media of RPE cells prepared from AMD and normal donors.

Other secreted proteins that were found to be increased in AMD RPE cells versus healthy RPE cells included galectin-3 binding protein, fibronectin, and lumican. Fibronectin and galectin-3 binding protein are known to promote integrin-mediated cell adhesion while lumican acts like collagen to form the extracellular matrix. The role of these proteins in AMD pathology and drusen biogenesis is not well understood. Nevertheless, fibronectin was previously reported to be more abundant in diffuse drusen which are the hallmark of AMD pathology than in nodular small drusen which are more ubiquitous retinal deposits.[64,65] Additionally, galectin-3 binding protein, also known as Human Mac-2 binding protein, was found to bind to a variety of extracellular proteins including fibronectin itself,[66] and it may therefore be relevant to analyze drusen for the presence of galectin 3 binding protein in drusen in future investigations.

Conclusion

The survey of secreted proteins in RPE cells was greatly facilitated by the use of the SILAC strategy. Because secreted proteins are labeled with heavy stable isotope amino acids, they can be easily distinguished from bovine serum contaminants that may be present in the spent media. In our case, even after washing the cells twice with PBS before incubation in serum-free media, we still detected several bovine serum proteins. Using this strategy in combination with SDS-PAGE, LC−MS/MS, and ZoomQuant analysis, several specific RPE secreted proteins were identified, and their level of expression was determined between cells prepared from AMD donors and cells prepared from age-matched healthy control donors. Secreted proteins have many important cellular functions, and their global analysis (secretomics) could bring insight into their role in pathological conditions such as AMD as well as other diseases involving angiogenesis and protein aggregation. Although these are ex vitro studies, the generated data could be used to select important proteins and follow their occurrence and activity in vivo.

Acknowledgment. This work was supported by a philanthropic donation to Dr. Hathout and by the Parson's Foundation. Financial support to Dr. Karl Csaky was provided by the NIH/NEI intramural program. E.A. thanks the Institute of Biomedical Sciences of George Washington University for their financial support. Eunkyung An is a predoctoral student in the Biochemistry and Molecular Genetics Program of the Institute for Biomedical Sciences at the George Washington University. This work is from a dissertation to be presented to the above program in partial fulfillment of the requirements for the Ph.D. degree. We also thank Dr. Kanneboyina Nagaraju for his advice and helpful discussion and Ms Stephanie Mitchell and Catherine Formolo for their help with manuscript editing.

References

(1) Evans, J. R. Risk factors for age-related macular degeneration. *Prog. Retinal Eye Res.* **2001**, *20*, 227−253.
(2) Young, R. W. Pathophysiology of age-related macular degeneration. *Surv. Ophthalomol.* **1987**, *31*, 291−306.
(3) van der Schaft, T. L.; de Bruijn, W. C.; Mooy, C. M.; de Jong, P. T. Basal laminar deposit in the aging peripheral human retina. *Graefes Arch. Clim. Exp. Ophthalmol.* **1993**, *231*, 470−475.
(4) Hageman, G. S.; Mullins, R. F. Molecular composition of drusen as related to substructural phenotype. *Mol. Vis.* **1999**, *3*, 25−28.
(5) Algvere, P. V.; Seregard, S. Drusen maculopathy: a risk factor for AMD. Can we prevent visual loss? *Acta Ophthalmol. Scand.* **2003**, *81*, 427−429.
(6) Bok, D. New insights and new approaches toward the study of age-related macular degeneration. *Proc. Natl. Acad. Sci. U.S.A.* **2002**, *99*, 14619−14621.
(7) Pauleikhoff, D.; Barondes, M.; Minassian, D.; Chrisholm, J.; Wessing, A.; Bird, A. C. Drusen and their significance in age related macular degeneration. *Fortschr. Ophthalmol.* **1990**, *87*, 429−432.
(8) Klein, R. J.; Zeiss, C.; Chew, E. Y.; Tsai, J. Y.; Sackler, R. S.; Haynes, C.; Henning, A. K.; SanGiovanni, J. P.; Mane, S. M.; Mayne, S. T.; Bracken, M. B.; Ferris, F. L.; Ott, J.; Barnstable, C.; Hoh, J. Complement factor H polymorphism in age-related macular degeneration. *Science* **2005**, *308*, 385−389.
(9) Edwards, A. O.; Ritter, R., 3rd; Abel, K. J.; Manning, A.; Panhuysen, C.; Farrer, L. A. Complement factor H polymorphism and age-related macular degeneration. *Science* **2005**, *308*, 421−424.
(10) Haines, J. L.; Hauser, M. A.; Schmidt, S.; Scott, W. K.; Olson, L. M.; Gallins, P.; Spencer, K. L.; Kwan, S. Y.; Noureddine, M.; Gilbert, J. R.; Schnetz-Boutaud, N.; Agarwal, A.; Postel, E. A.; Pericak-Vance, M. A. Complement factor H variant increases the risk of age-related macular degeneration. *Science* **2005**, *308*, 419−421.
(11) Hageman, G. S.; Anderson, D. H.; Johnson, L. V.; Hancox, L. S.; Taiber, A. J.; Hardisty, L. I.; Hageman, J. L.; Stockman, H. A.; Borchardt, J. D.; Gehrs, K. M.; Smith, R. J.; Silvestri, G.; Russell, S. R.; Klaver, C. C.; Barbazetto, I.; Chang, S.; Yannuzzi, L. A.; Barile, G. R.; Merriam, J. C.; Smith, R. T.; Olsh, A. K.; Bergeron, J.; Zernant, J.; Merriam, J. E.; Gold, B.; Dean, M.; Allikmets, R. A common haplotype in the complement regulatory gene factor H (HF1/CFH) predisposes individuals to age-related macular degeneration. *Proc. Natl. Acad. Sci. U.S.A.* **2005**, *102*, 7227−7232.
(12) Gold, B.; Merriam, J. E.; Zernant, J.; Hancox, L. S.; Taiber, A. J.; Gehrs, K.; Cramer, K.; Neel, J.; Bergeron, J.; Barile, G. R.; Smith, R. T.; Hageman, G. S.; Dean, M.; Allikmets, R.; Chang, S.; Yannuzzi, L. A.; Merriam, J. C.; Barbazetto, I.; Lerner, L. E.; Russell, S.; Hoballah, J.; Hageman. J.; Stockman, H. Variation in factor B (BF) and complement component 2 (C2) genes is associated with age-related macular degeneration. *Nat. Genet.* **2006**, *38*, 458−462.
(13) Farkas, T. G.; Sylvester, V.; Archer, D.; Altona, M. The histochemistry of drusen. *Am. J. Ophthalmol.* **1971**, *71*, 1206−1215.
(14) Boulton, M.; Dayhaw-Barker, P. The role of the retinal pigment epithelium: topographical variation and aging changes. *Eye* **2001**, *3*, 384−389.
(15) Tanihara, H.; Yoshida, M.; Matsumoto, M.; Yoshimura, N. Identification of transforming growth factor-beta expressed in cultured human retinal pigment epithelial cells. *Invest. Ophthalmol. Vis. Sci.* **1993**, *34*, 413−419.
(16) Alexander, J. J.; Pickering, M. C.; Haas, M.; Osawe, I.; Quigg, R. J. Complement factor h limits immune complex deposition and prevents inflammation and scarring in glomeruli of mice with chronic serum sickness. *J. Am. Soc. Nephrol.* **2005**, *16*, 52−57.
(17) Eichler, W.; Friedrichs, U.; Thies, A.; Tratz, C.; Wiedemann, P. Modulation of matrix metalloproteinase and TIMP-1 expression by cytokines in human RPE cells. *Invest. Ophthalmol. Vis. Sci.* **2002**, *43*, 2767−2773.
(18) Adamis, A. P.; Shima, D. T.; Yeo, K. T.; Yeo, T. K.; Brown, L. F.; Berse, B.; D'Amore, P. A.; Folkman, J. Synthesis and secretion of vascular permeability factor/vascular endothelial growth factor by human retinal pigment epithelial cells. *Biochem. Biophys. Res. Commun.* **1993**, *193*, 631−638.
(19) Murata, T.; Nakagawa, K.; Khalil, A.; Ishibashi, T.; Inomata, H.; Sueishi, K. The relation between expression of vascular endothelial growth factor and breakdown of the blood-retinal barrier in diabetic rat retinas. *Lab. Invest.* **1996**, *74*, 819−825.
(20) Ong, S. E.; Blagoev, B.; Kratchmarova, I.; Kristensen, D. B.; Steen, H.; Pandey. A.; Mann, M. Stable isotope labeling by amino acids in cell culture, SILAC, as a simple and accurate approach to expression proteomics. *Mol. Cell. Proteomics* **2002**, *1*, 376−86.
(21) Ong, S. E.; Foster, L. J.; Mann, M. Mass spectrometric-based approaches in quantitative proteomics. *Methods* **2003**, *29*, 124−130.
(22) Gehrmann, M. L.; Hathout, Y.; Fenselau, C. Evaluation of metabolic labeling for comparative proteomics in breast cancer cells. *J. Proteome Res.* **2004**, *3*, 1063−1068.
(23) Everley, P. A.; Krijgsveld, J.; Zetter, B, R.; Gygi, S. P. Quantitative cancer proteomics: stable isotope labeling with amino acids in cell culture (SILAC) as a tool for prostate cancer research. *Mol. Cell. Proteomics* **2004**, *3*, 729−35.
(24) Hathout, Y.; Flippin, J.; Fan, C.; Liu, P.; Csaky, K. Metabolic labeling of human primary retinal pigment epithelial cells for accurate comparative proteomics. *J. Proteome Res.* **2005**, *4*, 620−627.
(25) Ibarrola, N.; Kalume, D. E.; Gronborg, M.; Iwahori, A.; Pandey, A. A proteomic approach for quantitation of phosphorylation using stable isotope labeling in cell culture. *Anal. Chem.* **2003**, *75*, 6043−6049.
(26) Gruhler, A.; Schulze, W. X.; Matthiesen, R.; Mann, M.; Jensen, O. N. Stable isotope labeling of *Arabidopsis thaliana* cells and quantitative proteomics by mass spectrometry. *Mol. Cell. Proteomics* **2005**, *4*, 1697−709.
(27) Zhang, G.; Spellman, D. S.; Skolnik, E. Y.; Neubert, T. A. Quantitative Phosphotyrosine Proteomics of EphB2 Signaling by Stable Isotope Labeling with Amino Acids in Cell Culture (SILAC). *J. Proteome Res.* **2006**, *5*, 581−588.
(28) Blagoev, B.; Kratchmarova, I.; Ong, S. E.; Nielsen, M.; Foster, L. J.; Mann, M. A proteomics strategy to elucidate functional protein−protein interactions applied to EGF signaling. *Nat. Biotechnol.* **2003**, *21*, 315−318.

(29) Foster, L. J.; Rudich, A.; Talior, I.; Patel, N.; Huang, X.; Furtado, L. M.; Bilan, P. J.; Mann, M.; Klip, A. Insulin-dependent interactions of proteins with GLUT4 revealed through stable isotope labeling by amino acids in cell culture (SILAC). *J. Proteome Res.* **2006**, *5*, 64−75.
(30) Gronborg, M.; Kristiansen, T. Z.; Iwahori, A.; Chang, R.; Reddy, R.; Sato, N.; Molina, H.; Jensen, O. N.; Hruban, R. H.; Goggins, M. G.; Maitra, A.; Pandey, A. Biomarker discovery from pancreatic cancer secretome using a differential proteomic approach. *Mol. Cell. Proteomics* **2006**, *5*, 157−171.
(31) Alge, C. S.; Suppmann, S.; Priglinger, S. G.; Neubauer, A. S.; May, C. A.; Hauck, S.; Welge-Lussen, U.; Ueffing, M.; Kampik, A. Comparative proteome analysis of native differentiated and cultured dedifferentiated human RPE cells. *Invest. Ophthalmol. Vis. Sci.* **2003**, *44*, 3629−3641.
(32) Leschey, K. H.; Hackett, S. F.; Singer, J. H.; Campochiaro, P. A. Growth factor responsiveness of human retinal pigment epithelial cells. *Invest. Ophthalmol. Vis. Sci.* **1990**, *31*, 839−846.
(33) Livak, K. J. Allelic discrimination using fluorogenic probes and the 5′ nuclease assay. *Genet. Anal.* **1999**, *14*, 143−149.
(34) Halligan, B. D.; Slyper, R. Y.; Twigger, S. N.; Hicks, W.; Olivier, M.; Greene, A. S. ZoomQuant: an application for the quantitation of stable isotope labeled peptides. *J. Am. Soc. Mass. Spectrom.* **2005**, *16*, 302−306.
(35) Hittel, D. S.; Kraus, W. E.; Hoffman, E. P. Skeletal muscle dictates the fibrinolytic state after exercise training in overweight men with characteristics of metabolic syndrome. *J. Physiol.* **2003**, 548, 401−410.
(36) The Tumor Analysis Best Practices Working Group. Guidelines: Expression profiling − best practices for data generation and interpretation in clinical trials. *Nat. Rev. Gene.* **2004**, *5*, 229−237.
(37) Curcio, C. A.; Millican, C. L. Basal linear deposit and large drusen are specific for early age-related maculopathy. *Arch. Ophthalmol.* **1999**, *117*, 329−339.
(38) Gygi, S. P.; Rochon, Y.; Franza, B. R.; Aebersold, R. Correlation between protein and mRNA abundance in yeast. *Mol. Cell. Biol.* **1999**, *19*, 1720−1730.
(39) Tian, Q.; Stepaniants, S. B.; Mao, M.; Weng, L.; Feetham, M. C.; Doyle, M. J.; Yi, E. C.; Dai, H.; Thorsson, V.; Eng, J.; Goodlett, D.; Berger, J. P.; Gunter, B.; Linseley, P. S.; Stoughton, R. B.; Aebersold, R.; Collins, S. J.; Hanlon, W. A.; Hood, L. E. Integrated genomic and proteomic analyses of gene expression in Mammalian cells. *Mol. Cell. Proteomics* **2004**, *3*, 960−969.
(40) Gronborg, M.; Kristiansen, T. Z.; Iwahori, A.; Chang, R.; Reddy, R.; Sato, N.; Molina, H.; Jensen, O. N.; Hruban, R. H.; Goggins, M. G.; Maitra, A.; Pandey, A. Biomarker discovery from pancreatic cancer secretome using a differential proteomic approach. *Mol. Cell. Proteomics* **2006**, *5*, 157−171.
(41) Anderson, D. H.; Mullins, R. F.; Hageman, G. S.; Johnson, L. V. A role for local inflammation in the formation of drusen in the aging eye. *Am. J. Ophthalmol.* **2002**, *134*, 411−431.
(42) Hageman, G. S.; Luthert, P. J.; Victor Chong, N. H.; Johnson, L. V.; Anderson, D. H.; Mullins, R. F. An integrated hypothesis that considers drusen as biomarkers of immune-mediated processes at the RPE-Bruch's membrane interface in aging and age-related macular degeneration. *Prog. Retin. Eye. Res.* **2001**, *20*, 705−732.
(43) Malek, G.; Li, C. M.; Guidry, C.; Medeiros, N. E.; Curcio, C. A. Apolipoprotein B in cholesterol-containing drusen and basal deposits of human eyes with age-related maculopathy. *Am. J. Pathol.* **2003**, *162*, 413−425.
(44) Crabb, J. W.; Miyagi, M.; Gu, X.; Shadrach, K.; West, K. A.; Sakaguchi, H.; Kamei, M.; Masan, A.; Yan, L.; Rayborn, M. E.; Salomon, R. G.; Hollyfiend, J. G. Drusen proteome analysis: an approach to the etiology of age-related macular degeneration. *Proc. Natl. Acad. Sci. U.S.A.* **2002**, *99*, 14682−14687.
(45) Johnson, L. V.; Leitner, W. P.; Staples, M. K.; Anderson, D. H. Complement activation and inflammatory processes in Drusen formation and age related macular degeneration. *Exp. Eye. Res.* **2001**, *73*, 887−896.
(46) Alexander, J. J.; Pickering, M. C.; Haas, M.; Osawe, I.; Quigg, R. J. Complement factor h limits immune complex deposition and prevents inflammation and scarring in glomeruli of mice with chronic serum sickness. *J. Am. Soc. Nephrol.* **2005**, *16*, 52−57.
(47) Bailey, R. W.; Dunker, A. K.; Brown, C. J.; Garner, E. C.; Griswold, M. D. Clusterin, a binding protein with a molten globule-like region. *Biochemistry* **2001**, *40*, 11828−11840.
(48) Sakaguchi, H.; Miyagi, M.; Shadrach, K. G.; Rayborn, M. E.; Crabb, J. W.; Hollyfield, J. G. Clusterin is present in drusen in age-related macular degeneration. *Exp. Eye Res.* **2002**, *74*, 547−549.
(49) DeMattos, R. B.; O'dell, M. A.; Parsadanian, M.; Taylor, J. W.; Harmony, J. A.; Bales, K. R.; Paul, S. M.; Aronow, B. J.; Holtzman, D. M. Clusterin promotes amyloid plaque formation and is critical for neuritic toxicity in a mouse model of Alzheimer's disease. *Proc. Natl. Acad. Sci. U.S.A.* **2002**, *99*, 10843−10848.
(50) Anderson, D. H.; Talaga, K. C.; Rivest, A. J.; Barron, E.; Hageman, G. S.; Johnson, L. V. Characterization of beta amyloid assemblies in drusen: the deposits associated with aging and age-related macular degeneration. *Exp. Eye Res.* **2004**, *78*, 243−256.
(51) Luibl, V.; Isas, J. M.; Kayed, R.; Glabe, C. G.; Langen, R.; Chen, J. Drusen deposits associated with aging and age-related macular degeneration contain nonfibrillar amyloid oligomers. *J. Clin. Invest.* **2006**, *116*, 378−385.
(52) Rosenberg, M. E.; Silkensen, J. Clusterin: physiologic and pathophysiologic considerations. *Int. J. Biochem. Cell. Biol.* **1995**, *27*, 633−645.
(53) Plantner, J. J.; Jiang, C.; Smine, A. Increase in interphotoreceptor matrix gelatinase A (MMP-2) associated with age-related macular degeneration. *Exp. Eye Res.* **1998**, *67*, 637−645.
(54) Leu, S. T.; Batni, S.; Radeke, M. J.; Johnson, L. V.; Anderson, D. H.; Clegg, D. O. Drusen are Cold Spots for Proteolysis: Expression of Matrix Metalloproteinases and Their Tissue Inhibitor Proteins in Age-related Macular Degeneration. *Exp. Eye Res.* **2002**, *74*, 141−454.
(55) Lambert, V.; Wielockx, B.; Munaut, C.; Galopin, C.; Jost, M.; Itoh, T.; Werb, Z.; Baker, A.; Libert, C.; Krell, H. W.; Foidart, J. M.; Noel, A.; Rakic, J. M. MMP-2 and MMP-9 synergize in promoting choroidal neovascularization. *FASEB J.* **2003**, *17*, 2290−2292.
(56) Hiscott, P.; Hagan, S.; Heathcote, L.; Sheridan, C. M.; Groenewald, C. P.; Grierson, I.; Wong, D.; Paraoan, L. Pathobiology of epiretinal and subretinal membranes: possible roles for the matricellular proteins thrombospondin 1 and osteonectin (SPARC). *Eye* **2002**, *16*, 393−403.
(57) Chlenski, A.; Liu, S.; Crawford, S. E.; Volpert, O. V.; DeVries, G. H.; Evangelista, A.; Yang, Q.; Salwen, H. R.; Farrer, R.; Bray, J.; Cohn, S. L. SPARC is a key Schwannian-derived inhibitor controlling neuroblastoma tumor angiogenesis. *Cancer Res.* **2002**, *62*, 7357−7363.
(58) Nozaki, M.; Sakurai, E.; Raisler, B. J.; Baffi, J. Z.; Witta, J.; Ogura, Y.; Brekken, R. A.; Sage, E. H.; Ambati, B. K.; Ambati, J. Loss of SPARC-mediated VEGFR-1 suppression after injury reveals a novel antiangiogenic activity of VEGF-A. *J. Clin. Invest.* **2006**, *116*, 422−429.
(59) Sternlicht, M. D.; Werb, Z. How matrix metalloproteinases regulate cell behavior. *Annu. Rev. Cell. Dev. Biol.* **2001**, *17*, 463−516.
(60) Sage, E. H.; Reed, M.; Funk, S. E.; Truong, T.; Steadele, M.; Puolakkainen, P.; Maurice, D. H.; Bassuk, J. A. Cleavage of the matricellular protein SPARC by matrix metalloproteinase 3 produces polypeptides that influence angiogenesis. *J. Biol. Chem.* **2003**, *278*, 37849−37857.
(61) Dawson, D. W.; Volpert, O. V.; Gillis, P.; Crawford, S. E.; Xu, H.; Benedict, W.; Bouck, N. P. Pigment epithelium-derived factor: a potent inhibitor of angiogenesis. *Science* **1999**, *285*, 245−248.
(62) Martin, G.; Schlunck, G.; Hansen, L. L.; Agostini, H. T. Differential expression of angioregulatory factors in normal and CNV-derived human retinal pigment epithelium. *Graefes. Arch. Clin. Exp. Ophthalmol.* **2004**, *242*, 321−326.
(63) Gao, G.; Li, Y, Gee, S.; Dudley, A.; Fant, J.; Crosson, C.; Ma, J. X. Down-regulation of vascular endothelial growth factor and up-regulation of pigment epithelium-derived factor: a possible mechanism for the anti-angiogenic activity of plasminogen kringle 5. *J. Biol. Chem.* **2002**, *277*, 9492−9497.
(64) Newsome, D. A.; Hewitt, A. T.; Huh, W.; Robey, P. G.; Hassell, J. R.; Detection of specific extracellular matrix molecules in drusen, Bruch's membrane, and ciliary body. *Am. J. Ophthalmol.* **1987**, *104*, 373−381.
(65) Grossniklaus, H. E.; Martinez, J. A.; Brown, V. B.; Lambert, H. M.; Sternberg, P. Jr.; Capone, A., Jr.; Aaberg, T. M.; Lopez, P. F. Immunohistochemical and histochemical properties of surgically excised subretinal neovascular membranes in age-related macular degeneration. *Am. J. Ophthalmol.* **1992**, *114*, 464−472.
(66) Sasaki, T.; Brakebusch, C.; Engel, J.; Timpl, R. Mac-2 binding protein is a cell-adhesive protein of the extracellular matrix which self-assembles into ring-like structures and binds beta1 integrins, collagens and fibronectin. *EMBO J.* **1998**, *17*, 1606−1613.

PR060121J